Measurement method for electric fields based on Stark spectroscopy of argon atoms

V. P. Gavrilenko,* H. J. Kim,† T. Ikutake, J. B. Kim, Y. W. Choi,‡ M. D. Bowden,§ and K. Muraoka
Interdisciplinary Graduate School of Engineering Sciences, Kyushu University, Kasuga Fukuoka 816-8580, Japan
(Received 11 April 2000)

We report the development of a method for the measurement of electric fields in glow discharge plasmas, based on Stark spectroscopy of argon atoms. The method is based on laser excitation of transitions in atomic argon. The key feature of the method is that the electric field is determined by matching experimentally obtained absorption spectra to theoretically calculated spectra. The dependence of the positions of energy levels of argon atoms on the strength of the electric field was calculated by solving the Schrödinger equation for the argon atom. Measurements of Stark spectra were made in the sheath region of a glow discharge using laser optogalvanic spectroscopy. The wavelength of the laser radiation was tuned to the transitions $4s \Rightarrow nf$ ($n=7,8,\ldots,14$) of the argon atom. For $n=11$, the lower limit for electric field measurements was estimated to be 14 V/mm.

PACS number(s): 52.70.−m, 32.60.+i, 52.80.−s

I. INTRODUCTION

The electric field in a gas discharge is one of the most important discharge parameters. In glow discharges, it is closely connected with other discharge parameters such as charge densities, energy distribution functions, and fluxes of ions and electrons. The spatial distribution of the electric fields throughout the whole discharge, and especially in the sheath regions near electrodes and material surfaces, serves as input data for plasma discharge modeling. For these reasons, studying spatial distribution of electric fields in the discharge is of great practical importance.

One of the main techniques for measurements of electric fields in discharges is based on the Stark effect of species (atoms and molecules), which either are present in a discharge or are added to the discharge for the purpose of diagnostics. Techniques have been developed for glow discharges containing hydrogen [1,2] and helium [3–10], using either shifts and/or splitting of energy levels due to Stark effects. Other techniques based on Stark mixing of energy levels have been developed for discharges containing BCl [11–13], NaK [14–15], and CS [16]. For hydrogen and helium, the determination of electric field was based on a theoretical calculation of the Stark effect. For other species, some kind of calibration was necessary to rigorously correlate the experimentally observed Stark effects with the electric field intensity.

There is a strong need for techniques that can measure electric field distributions in discharges in gases such as argon, which is widely used for plasma processing. We previously reported on the development of a technique based on spectroscopy of argon atoms, and suitable for application in glow discharges [17,18]. In these papers, the Stark shift of several allowed spectral lines of argon was calibrated experimentally against a discharge electric field that was obtained in turn from spectra of helium atoms. In addition, it was also observed [18] that for the transitions to the Rydberg energy levels of argon atoms, there appear many forbidden spectral lines, the positions of which strongly depended on the strength of the electric field.

In this paper, we describe research that significantly improves the sensitivity and the detection limit of this electric field measurement method. This was achieved by a combination of examining transitions in argon atoms that are much more sensitive to the electric field than those previously studied, and most importantly, by theoretically calculating the dependence of argon energy levels on the electric field. It is important to have a quantitative description of the Stark effect for argon atoms in order to obtain the electric field dependencies of the positions of argon spectral lines, both allowed and forbidden. Such a quantitative description can be used as the basis of a technique for the direct measurement of electric fields in argon discharges, without the need for an experimental calibration procedure. The quantitative description described in this paper improved the measurement accuracy because the rather large experimental uncertainties associated with the previous calibration are replaced by much smaller uncertainties associated with the theoretical calculation. The detection limit for the electric field was improved because transitions to Rydberg levels with higher principal quantum number n were studied.

This research consists of two main parts. In the first part, we measured absorption spectra of laser radiation for transitions from the metastable level $4s[\frac{3}{2}]_2$ to Rydberg levels characterized by principal quantum numbers $n=7,\ldots,14$. The measurements were made in the sheath region of a dc glow discharge operated in argon. In the second part, we calculated absorption spectra, based on a solution of the Schrödinger equation for the argon atom being in Rydberg state and interacting with an electric field. These two studies

*Permanent address: Center for Surface and Vacuum Research, Russian State Committee for Standards, Andreyevskaya nab. 2, Moscow 117334, Russia.

†Permanent address: Samsung SDI Co. Ltd., 508 Sungsung-Dong, Chonan City, Chungchongnam-Do, 330-300, Korea.

‡Permanent address: Korea Electrotechnology Research Institute, Changwon 641-600, Korea.

§Author to whom correspondence should be addressed. Email address: bowden@asem.kyushu-u.ac.jp

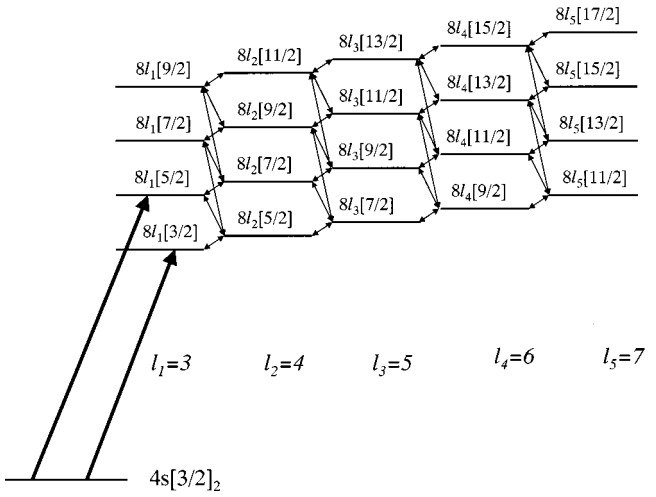

FIG. 1. Partial scheme of energy levels of an argon atom. The laser radiation populated levels of the principal quantum number $n=8$ by excitation from the lower level $4s[\frac{3}{2}]_2$ (thick arrows). Thin arrows indicate the Stark coupling of energy levels due to the effect of the electric field. Each energy level of $n=8$ consists of a pair of closely spaced sublevels corresponding to two different values of the total angular momentum J: $J_1=K-\frac{1}{2}, J_2=K+\frac{1}{2}$, where the quantum number K is indicated in brackets above the corresponding energy level.

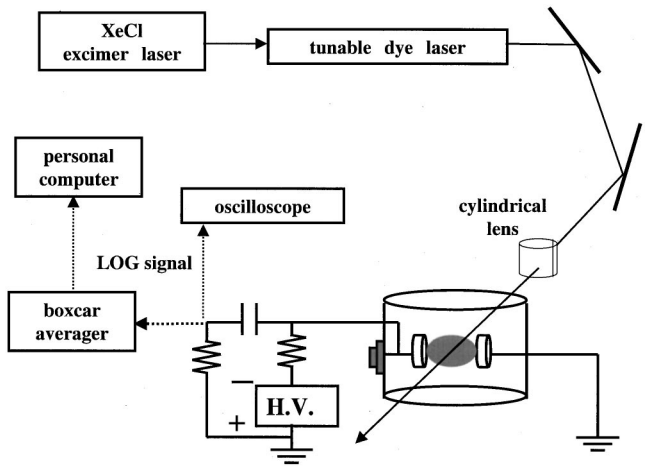

FIG. 2. Experimental system used for LOG measurements in a dc glow discharge.

are described below in Secs. II and III, respectively. Section IV contains a comparison of the experimental and theoretical results. Section V contains a description of how the discharge electric field can be determined with this method, and a discussion of the measurement accuracy and detection limits. Section VI is a brief summary.

II. EXPERIMENTAL METHOD AND RESULTS

The spectroscopic scheme is shown in Fig. 1. Laser excitation was used to excite argon atoms from the $4s[\frac{3}{2}]_2$ metastable level to Rydberg levels. In the absence of an electric field, the only allowed transitions are those from the metastable level to the $nf[\frac{5}{2}]_{2,3}$ and $nf[\frac{3}{2}]_{1,2}$ levels. These transitions are shown in the figure by the solid arrows.

The experimental apparatus is shown in Fig. 2. The laser source was a tunable dye laser pumped by a xenon chloride excimer laser. The laser was operated at $\lambda \sim 600$ nm, and the laser output was frequency doubled to generate the radiation at $\lambda \sim 300$ nm which was used for the excitation. The output of the dye laser had pulse duration of 25 ns and a spectral width of 0.2 cm^{-1}. A cylindrical lens was used to focus the laser beam into a sheetlike beam with a width of 0.1 mm and a height of 2 mm. The beam was directed through the plasma parallel to the electrode surfaces. Measurements were performed by scanning the dye laser wavelength and measuring the absorption spectrum by laser optogalvanic (LOG) spectroscopy.

Figures 3(a), 3(c), 3(e), 3(g), 3(i), 3(k), 3(m), and 3(o) show the LOG spectra measured for transitions from the lower level $4s[\frac{3}{2}]_2$ to Rydberg levels with principal quantum numbers $n=7,\ldots,14$. These spectra were obtained from discharge plasmas with pressures of 5.0 ± 0.2 torr. Each set of measurements shows spectra measured when the laser was at different distances from the cathode surface. The distance d shown in the figure is the distance from the cathode surface, the position of which corresponds to $d=0$ mm.

Spectra obtained when the laser beam was far from the cathode show only two peaks, corresponding to the transitions from the level $4s[\frac{3}{2}]_2$ to levels $nf[\frac{5}{2}]_{2,3}$ and $nf[\frac{3}{2}]_{1,2}$. (The wavelengths of these transitions are shown in Table I). Spectra obtained when the laser beam was in the vicinity of the cathode show many peaks. This strong restructuring of the absorption spectrum is due to the Stark effect caused by the electric field near the cathode. Although the main features of the Stark effect for Rydberg levels of argon atoms are considered theoretically in Sec. III, important features of the experimental spectra are discussed briefly here.

It should be noted that for excitation to $n=7,\ldots,12$, spectra are shown for positions ranging from close to the electrode, where the electric field is high, to far from the electrode, corresponding to outside the sheath. For excitation to $n=13$ and 14, however, spectra are shown only for positions in the outer parts of the sheath, where the electric field is relatively small. This is because the high sensitivity of these levels to the electric field, together with the relatively small energy difference between adjacent energy levels, means that at high electric field, the spectra from adjacent levels overlap. This leads to very confused spectra.

The spectra for excitation to $n=7$, 8, and 9 levels are similar to those reported previously [18]. It can be seen from the whole set of spectra that, as expected, levels with higher n are much more sensitive to the electric field. This sensitivity of the levels with high n can be seen clearly by directly comparing spectra obtained at the same spatial position. The spectra obtained at $d=1.0$ mm for excitation to $n=7$ is essentially identical to that obtained at $d=1.5$ mm, outside the sheath. Spectra obtained at similar positions using excitation to $n=14$, however, are completely different. This and other important aspects of the experimental spectra are discussed in Secs. IV and V.

Another feature of the spectra is that, when many peaks are present in the spectrum, the outer peaks are spectrally broader than the central peaks. This broadening is due to the finite range of electric field that exists within the laser beam cross section, and is discussed further in Sec. III.

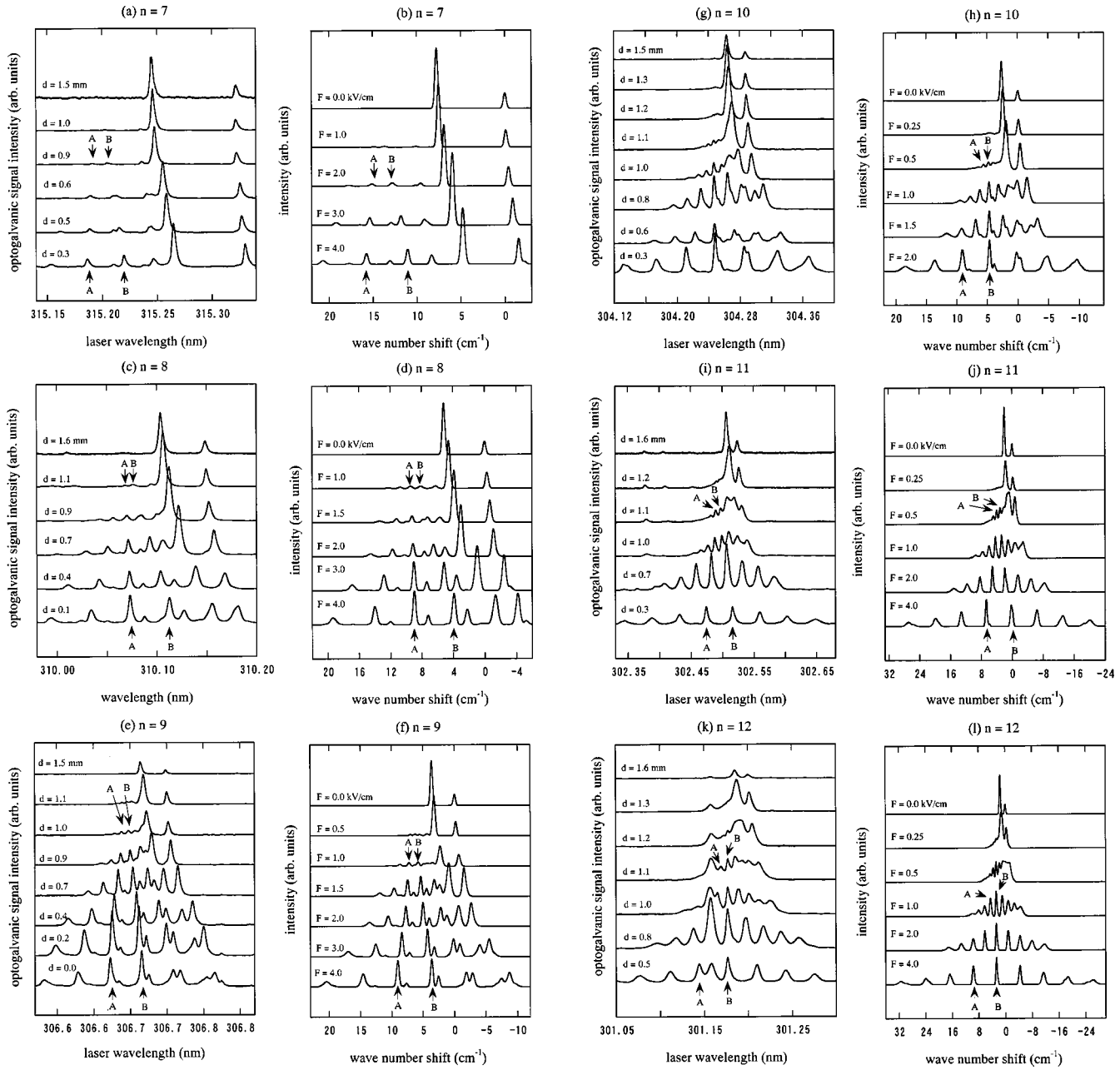

FIG. 3. (a), (c), (e), (g), (i), (k), (m), and (o) Experimental LOG spectra obtained at different distances from the cathode in an argon discharge at 5.0 Torr. (b), (d), (f), (h), (j), (l), (n), and (p) Theoretical spectra of absorption of laser radiation at transitions between the lower level $4s[\frac{3}{2}]_2$ and the upper levels of principal quantum number n of argon atoms ($n=7,8,\ldots,14$). Each pair of spectra corresponds to excitation to levels with different n. For both experimental and theoretical spectra, the vector of polarization of the laser radiation was parallel to the discharge electric field.

III. THEORETICAL CALCULATION AND RESULTS

A. Theory of the Stark effect for Rydberg levels of argon atoms

For Rydberg states of an argon atom, the $(j1)$ coupling scheme can be applied [19,20]. Within this scheme, the strong coupling of the orbital momentum of the Rydberg electron $\mathbf{l}$ to the ion-core total angular momentum j_c produces the angular momentum $\mathbf{K}=\mathbf{j}_c+\boldsymbol{l}$. The angular momentum $\mathbf{K}$ is weakly coupled to the Rydberg electron spin $\mathbf{s}$. The total angular momentum of the whole argon atom is $\mathbf{J}=\mathbf{K}+\mathbf{s}$. Therefore, in our consideration of the Stark effect of argon atoms, we use the basis wave functions of energy levels of argon atoms in the form $\varphi=|nl[K]_J\rangle$ where n is the principal quantum number of the Rydberg electron.

In order to find the wave functions and the positions of energy levels of Rydberg states of argon atoms, we numerically solve the following Schrödinger equation for argon atoms interacting with the electric field $\mathbf{F}$:

$$H\psi=\varepsilon\psi, \quad H=H_0+ezF. \tag{1}$$

In this expression, H_0 is the unperturbed Hamiltonian of an argon atom, and ezF is the operator of the dipole interaction of the argon atom with the electric field $\mathbf{F}$. The axis z is

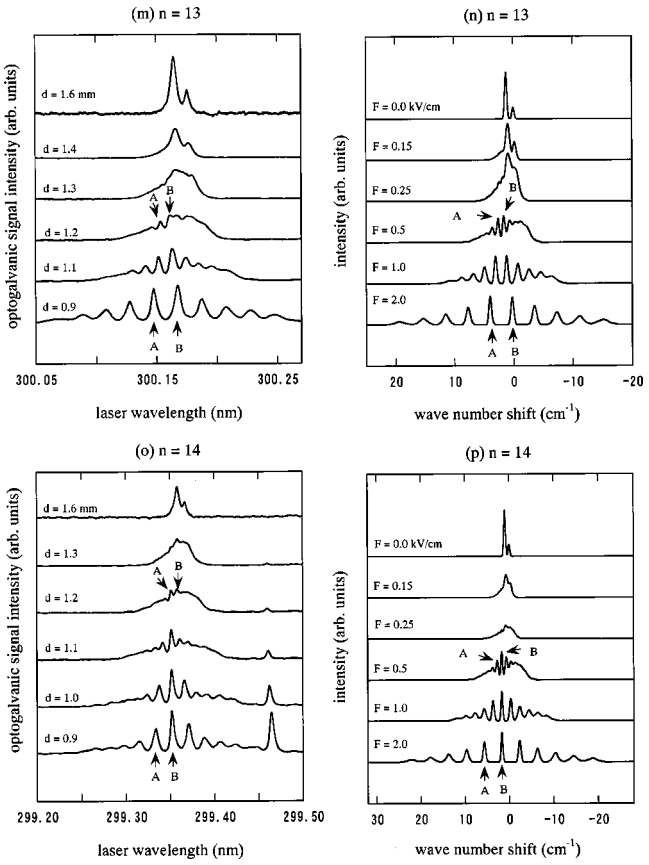

FIG. 3. (*Continued.*)

chosen to be parallel to the direction of the vector **F**. The matrix H_0 is diagonal, its elements being unperturbed energies of argon levels. The off-diagonal elements of the operator z are

$$\langle (nlj_c)KsJM|z|(n'l'j_c)K'sJ'M'\rangle = (-1)^{J+J'+K+K'+l+j_c+s-M}[(2J+1)(2J'+1)(2K+1)\times(2K'+1)]^{1/2}\delta_{MM'}\begin{pmatrix} J & 1 & J' \\ -M & 0 & M \end{pmatrix}\begin{Bmatrix} K & J & s \\ J' & K' & 1 \end{Bmatrix}\times\begin{Bmatrix} l & K & j_c \\ K' & l' & 1 \end{Bmatrix}\langle nl\|r\|n'l'\rangle,$$

TABLE I. Wavelengths of the allowed transitions from the $4s[\frac{3}{2}]_2$ metastable state to the nf states.

Upper level	$[\frac{5}{2}]_2$	$[\frac{3}{2}]_2$
$7f$	315.245 nm	315.322 nm
$8f$	310.104 nm	310.149 nm
$9f$	306.665 nm	306.702 nm
$10f$	304.261 nm	304.287 nm
$11f$	302.503 nm	302.521 nm
$12f$	301.185 nm	301.191 nm
$13f$	300.160 nm	300.165 nm
$14f$	299.354 nm	299.358 nm

where $j_c=\frac{3}{2}$, $s=\frac{1}{2}$, M is the quantum number of the projection of **J** onto the axis z, $\delta_{MM'}$ is the Kronecker symbol, $\begin{pmatrix} j_1 & j & j_2 \\ m_1 & m & m_2 \end{pmatrix}$ is the $3j$ symbol, $\begin{Bmatrix} j_1 & j_2 & j_3 \\ l_1 & l_2 & l_3 \end{Bmatrix}$ is the $6j$ symbol, and $\langle nl\|r\|n'l'\rangle$ is the reduced matrix element:

$$\langle nl\|r\|n'l'\rangle=\begin{cases} -(l+1)^{1/2}\langle nl|r|n',l+1\rangle, & l'=l+1 \\ l^{1/2}\langle nl|r|n',l-1\rangle, & l'=l-1. \end{cases}$$

The radial matrix elements $\langle n,l+1|r|nl\rangle$, which are needed for calculating the Stark splitting of upper levels nl (with $l\geqslant 3$), can be calculated using the tables presented in Ref. [21]. Our analysis has shown that these matrix elements are close to those given by the hydrogenic formula [22]

$$\langle n,l+1|r|nl\rangle=(3n/2)[n^2-(l+1)^2]^{1/2}a_0,$$

where a_0 is the Bohr radius. This is due to the fact that for the nl configurations with $l\geqslant 3$, the quantum defects δ_1 are small (i.e., $\delta_1\ll 1$). Therefore, we used the hydrogenic formula, shown above, for the matrix elements $\langle n,l+1|r|nl\rangle$ with $l\geqslant 3$ while solving Eq. (1). We also took into account the following selection rules for the Stark mixing of energy levels of an argon atom:

$$\Delta J=\pm 1 \quad \text{for} \quad M=0, \quad \Delta J=0,\pm 1 \quad \text{for} \quad M\neq 0,$$

$$\Delta K=0,\pm 1, \quad \Delta l=\pm 1. \tag{2}$$

Since the initial state $4s[\frac{3}{2}]_2$ has a small admixture of the state $3d[\frac{3}{2}]_2$ laser excitation can populate nf Rydberg states of argon atoms. The selection rules in Eq. (2) are also applicable for such a laser excitation. From these selection rules, we can conclude that within nf Rydberg levels of the same n, only two fine-structure doublets $nf[\frac{3}{2}]_{1,2}$ and $nf[\frac{5}{2}]_{2,3}$ can be populated by laser radiation in the absence of an electric field **F**. These two components, corresponding to the transitions $4s[\frac{3}{2}]_2\rightarrow nf[K]_J$ ($K=\frac{3}{2}$ and $\frac{5}{2}$), were observed in the experimental LOG spectra far from the cathode shown in Fig. 2. When $\mathbf{F}\neq 0$, the wave functions of the levels $nl[K]_J$ having the same n are intermixed. This leads to the appearance of a large number of Stark components in the LOG spectrum of argon atoms in the electric field. The vector of polarization of the laser radiation is parallel to **F** in our experiment. Therefore, the laser radiation couples the states $4s[\frac{3}{2}]_2$ and $nf[K]_J$ having the same quantum number M ($|M|=0$, 1, and 2). We solved Eq. (1) by performing a numerical diagonalization of the matrix $H=H_0+ezF$ for each value of M ($M=0$, ± 1, and ± 2). The matrix H has the dimension $(8n-24)\times(8n-24)$. The solution of Eq. (1) can be written in the form

$$\psi_\mu^{(n,M)}(F)=\sum_{l=3}^{n-1}\sum_{K,J}Q_{\mu,lKJ}^{(n,M)}(F)|nl[K]_J,M\rangle,$$

$$\mu=1,2,\ldots,8n-24, \tag{3}$$

where coefficients $Q_{\mu,lKJ}^{(n,M)}(F)$ are obtained as a result of the diagonalization of the matrix H.

Let us assume that the Zeeman states with different M ($M=0$, ±1, and ±2) of the lower level $4s[\frac{3}{2}]_2$ are equally populated, and that there is no saturation for the laser excitation. The intensities of the Stark components in the LOG spectrum for the fixed magnitude of the electric field F then can be expressed as

$$I_\mu(F)=P_L\sum_{M=-2}^{+2}|\langle 3d[\tfrac{3}{2}]_2,M|z|\psi_\mu^{(n,M)}(F)\rangle|^2,$$

$$\mu=1,2,\ldots,8n-24, \tag{4}$$

where the coefficient P_L is proportional to the intensity of the laser radiation and is independent of the values of F and μ. The positions $\varepsilon_\mu(F)$ of Stark components in the LOG spectrum having the intensity $I_\mu(F)$ are the eigenvalues of the Hamiltonian H [see Eq. (1)]. These eigenvalues also are obtained as a result of diagonalization of the matrix H.

B. Effect of the electric field gradient

As noted in Sec. II in the experimental LOG spectra recorded in the vicinity of the cathode, the profiles of the outer Stark components are broader than those of the central components. This indicates that the electric fields were inhomogeneous within the cross section of the laser beam because of the electric field gradient. Such a difference of the widths of the outer and central components of the experimental LOG spectra can be explained by the combination of two factors. First, for the inhomogeneous electric fields, the different argon atoms within the cross section of the laser beam are under the action of the electric fields of different magnitudes. Second, for the spectrum of argon atoms, when the magnitude of the electric field F varies, the corresponding change of the positions of the central Stark components is smaller than that of the outer Stark components. This effect of the electric field gradient has been observed previously in spectral lines of helium, reported in Refs. [3] and [4].

Theoretically, we describe the effect of the inhomogeneous electric fields by considering a distribution function of the electric fields $W(F)$, the value $W(F)dF$ being the probability for the magnitude of the electric field F to be within the small range from F to $F+dF$. Using the distribution function $W(F)$, the Stark profile of each spectral component can be represented as

$$S_\mu(\Delta\varepsilon)=\int_{-\infty}^{+\infty}G_\mu^{(F)}(\Delta\varepsilon)W(F)dF,\quad \Delta\varepsilon=\varepsilon-\varepsilon_\mu(F). \tag{5}$$

Here $\varepsilon_\mu(F)$ is the position of the spectral component having an intensity $I_\mu(F)$, and $G_p^{(F)}(\Delta\varepsilon)$ is the profile of this component. For the profile $G_\mu^{(F)}(\Delta\varepsilon)$, we use a Gaussian with full width at half maximum (FWHM) equal to 0.004 nm. This value of the FWHM was obtained from the experimental LOG spectra recorded far from the cathode (where the Stark broadening of spectral lines was small). The good agreement between the experimental and theoretical LOG spectra is achieved when we use the electric field distribution function

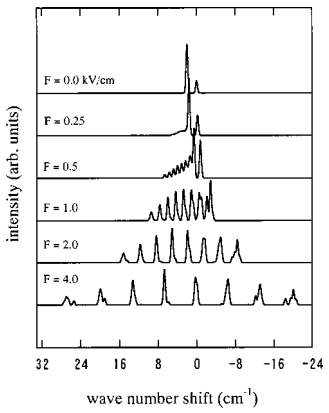

FIG. 4. The same as in Fig. 3(j), but without integrating over the electric field distribution function $W(F)$.

$$W(F)=\begin{cases}\dfrac{\delta F_{1/2}}{2\pi A_0}\dfrac{1}{(F-F_0)^2+(\delta F_{1/2}/2)^2}, & |F-F_0|<3\,\delta F_{1/2}/2\\ 0, & |F-F_0|\geqslant 3\,\delta F_{1/2}/2,\end{cases} \tag{6}$$

where F_0 is the mean magnitude of the electric field ($F_0>0$), the value of $\delta F_{1/2}$ is given by the relation

$$\delta F_{1/2}=\begin{cases}2F_0/3, & 0<F_0<0.24\ \text{kV/cm}\\ 0.16\ \text{kV/cm}, & F_0\geqslant 0.24\ \text{kV/cm},\end{cases}$$

and $A_0\approx 2\pi^{-1}\arctan 3\approx 0.7952$. Thus, for $|F-F_0|<3\,\delta F_{1/2}/2$, the distribution function $W(F)$ in Eq. (6) has the form of a Lorenzian profile, the value of $\delta F_{1/2}$ being the FWHM of the profile $W(F)$. The coefficient A_0 is introduced in Eq. (6) in order to satisfy the normalization condition

$$\int_{-\infty}^{+\infty}W(F)dF=1.$$

Figures 3(b), 3(d), 3(f), 3(h), 3(j), 3(l), 3(n), and 3(p) show the theoretical spectra obtained for the various magnitudes of the mean electric field F_0. These spectra correspond to the transitions to the energy levels of argon atoms corresponding to $n=7,\ldots,14$. These theoretical spectra were calculated using Eqs. (4)–(6).

IV. COMPARISON OF EXPERIMENTAL AND THEORETICAL SPECTRA

The experimental spectra shown in Fig. 3 were measured at different distances from the electrode, and so each group of spectra represents a set measured at regular intervals in a region with a monotonically increasing electric field. The theoretical spectra shown in Fig. 3 were calculated for different, regularly spaced, electric field magnitudes. It can be seen that there is good agreement between the experimental and theoretical spectra. Both the intensity and spectral position of the different Stark components agree very well.

The theoretical spectra were calculated including the effects of the distribution of electric field within the laser beam cross-section, as discussed in Sec. III B. Figure 4 shows the-

oretical spectra for excitation to $n=11$ that were calculated *without* this effect. Comparing the theoretical spectra presented in Figs. 3(j) and 4, we can conclude that integrating over the distribution function of the electric fields $W(F)$ is important in order to describe the experimental LOG spectra correctly.

For some cases, the experimental spectra contain some additional spectral lines. For instance, for excitation to $n=12$, there is a strong additional line at the wavelength $\lambda \sim 300.96$ nm, and for excitation to $n=14$, there is one at $\lambda \sim 299.26$ nm. These accessory lines, however, do not interfere with the determination of electric field.

An interesting feature of both the experimental and theoretical spectra with $n \geqslant 9$ is that, for high electric fields, these spectra consist of equidistantly spaced Stark components, the number of such Stark components being $N=n-3$. This result can be understood by taking into account the fact that for high electric fields, when the Stark interaction of the argon atom with the electric field exceeds the separation of the energy sublevels corresponding to the principal quantum number n, the Stark effect of the argon atom can be considered as the Stark effect in the system of the degenerated levels nl where $l=3,4,\ldots,n-1$. There are $n-3$ such levels, and, hence, the number of Stark components should be also equal to $n-3$.

It should be noted that spectra similar to that presented in Fig. 3 were obtained experimentally and calculated theoretically in the work of Ref. [23] for the transition to the upper level $n=18$ in argon. In this work, a collinear laser spectroscopic technique was applied to an atomic beam of argon.

V. DETERMINATION OF THE ELECTRIC FIELD DISTRIBUTION

It can be seen from Fig. 3 that, for sufficiently strong electric fields, the Stark spectra consist of many components. The positions of most of these components depend strongly on the magnitude of the electric field. These dependencies can be used for the measurement of the electric field in a discharge in two ways.

For the measurement of moderate electric fields, it is convenient to use the separation between the two closely spaced spectral lines that are indicated in Figs. 3 and 4 by letters A and B, to determine the magnitude of the electric field. These lines correspond to the dipole-forbidden transitions, and they appear in the spectra only due to the Stark mixing of the wave functions belonging to various sublevels of the upper energy level. Figure 5 shows the dependencies of the separation between these forbidden lines A and B on the strength of the electric field F_0, calculated for the transitions from the $4s[\frac{3}{2}]_2$ level to the $n=7,\ldots,14$ levels. As the distribution function of the electric fields, we used the function $W(F)$ presented in Eq. (6).

When the electric field is very weak and the separation between the forbidden components cannot be measured accurately, the magnitude of the electric field can be deduced from the small Stark shift of the allowed spectral lines corresponding to the transitions $4s[\frac{3}{2}]_2 \rightarrow nf[K]$, where $K=\frac{3}{2}$ and $\frac{5}{2}$. This shift is approximately a quadratic function of the strength of the electric field. Figure 6 shows the dependencies of the shift of the allowed spectral line on the strength of the electric field F_0, calculated for the transitions from the $4s[\frac{3}{2}]_2$ level to the $n=7,\ldots,11$ levels. For excitation to higher levels, the spectral peaks due to allowed transitions are extremely close together, and the shift of a single peak could not be determined accurately.

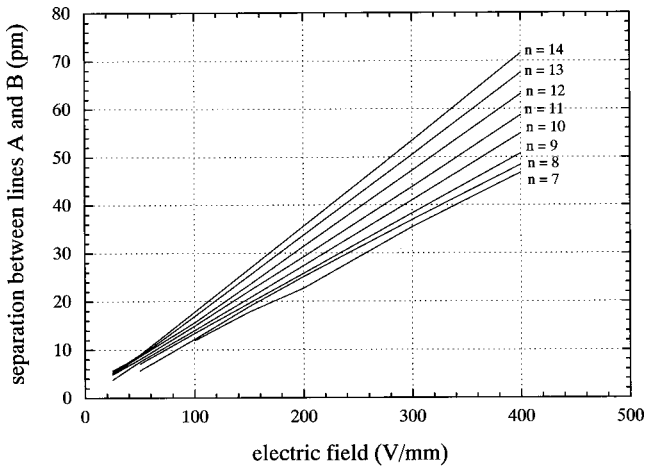

FIG. 5. The dependencies of the separation between the two closely spaced spectral lines indicated in Fig. 3 by letters A and B on the magnitude of the electric field F_0 calculated for transitions from the lower energy level $4s[\frac{3}{2}]_2$ to the upper levels of the principal quantum numbers $n=7,8,\ldots,14$ of argon atoms.

Figure 7 shows the spatial distribution of the electric field in the cathode region of the discharge, determined from experimental spectra. This distribution was obtained using the experimental LOG spectra corresponding to transitions from the lower metastable level $4s[\frac{3}{2}]_2$ to upper levels corresponding to $n=10$ and 11. For distances from the cathode in the range $0 \leqslant d \leqslant 1.2$ mm, the magnitude of the electric field F_0 was deduced from the dependence of the separation between lines A and B on F_0. For $d \geqslant 1.3$ mm, where the electric field is extremely weak, the value of F_0 was deduced from the Stark shift of the allowed spectral lines $4s[\frac{3}{2}]_2$

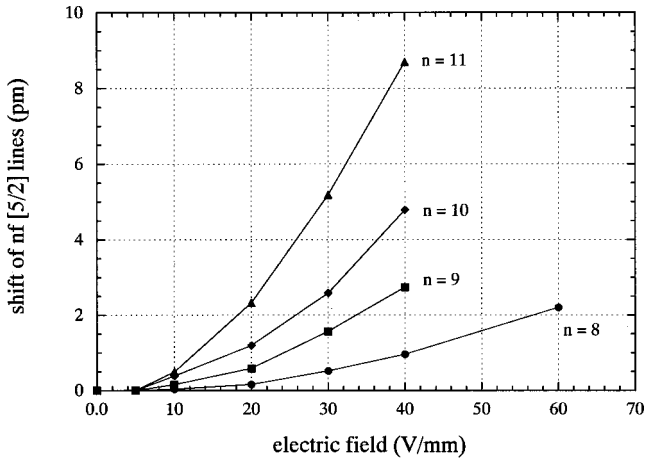

FIG. 6. The dependence of the shift of the allowed transition for weak electric fields. The shift is defined as being $\Delta\lambda=\lambda-\lambda_0$, where λ is the wavelength of the observed peak, and λ_0 is the wavelength of the peak when the electric field F_0 is zero.

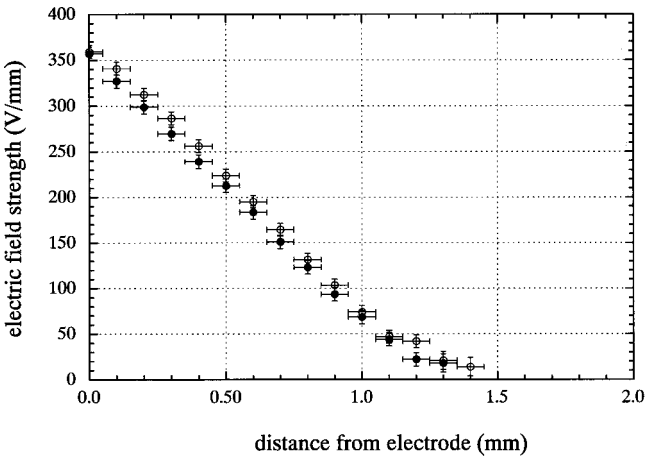

FIG. 7. The electric field spatial distribution measured in the vicinity of the cathode.

$\rightarrow nf[\frac{5}{2}]$, where $n=10$ and 11. The voltage drop across the cathode sheath can be calculated by integrating the field distribution shown in Fig. 7. In this case, the magnitude of the integrated voltage across the gap from 0.0 to 1.2 mm was 220 ± 10 V, which represents about 90% of the voltage of 250 ± 5 V that was applied across the discharge.

An interesting feature of the electric field distribution shown in Fig. 7 is that the field appears to taper off gradually rather than decrease linearly to zero at the sheath edge. This feature may be an indication of the start of the presheath region. Further measurements aimed at resolving this region more clearly are planned.

The detection uncertainties and the lower detection limit of this method of electric field measurement can be estimated from the results shown here. The accuracy of the electric field determined from any given spectrum is determined by a combination of the accuracy to which the spectral positions could be measured and the sensitivity of that transition to the electric field. In this experiment, the accuracy of the wavelength measurement is determined mainly by the spectral width of the laser. The sensitivity of transitions to the electric field is different for large electric fields, for which the dependence is approximately linear, and small electric fields, for which the dependence is approximately quadratic. Hence the measurement uncertainties are different for large and small electric fields.

We first consider the case of sufficiently large electric fields. Of the transitions studied here, excitation to $n=14$ is the most sensitive, and for the dye laser source used here (a spectral width of 0.2 cm^{-1}) the electric field could be determined with an uncertainty of ±6 V/mm. The errors bars shown in the Fig. 7, for excitation to $n=10$ and 11, correspond to ±7 V/mm.

For small electric fields, less than ~25 V/mm, all the transitions have a relatively weak dependence on the electric field. The error bars shown in Fig. 7 for these fields, at positions of $d\geqslant1.2$ mm, correspond to ±10 V/mm.

The lower detection limit for an electric field is determined by the same factors mentioned above for the measurement of small electric fields. In this experiment, the lowest electric field that we measured was 14 V/mm, determined using the shift of the allowed transition to the $n=11f$ levels.

VI. SUMMARY AND CONCLUSION

In conclusion, we report a spectroscopic method for measurement of the magnitude of the electric field in a glow discharge in argon. The method is based on measuring the dependence of the positions and intensities of spectral components in the LOG spectra of argon atoms on the magnitude of the electric field. These parameters of the LOG spectra were calculated by solving the Schrödinger equation for the argon atoms. The LOG spectra correspond to laser excitation from the metastable level $4s[\frac{3}{2}]_2$ to Rydberg levels of argon atoms. Using this method, we measured the spatial distribution of the electric field in the cathode region of a glow discharge with high accuracy. Although the LOG method was used to detect absorption spectra in this experiment, it should be noted that LIF detection also is possible [7,17,18].

Measurements to high Rydberg levels and the use of theoretical calculations of Stark spectra of argon atoms enabled us to significantly improve both the physical understanding and the practical implementation of this electric field measurement technique. With our current understanding of the Stark spectra, and existing experimental apparatus, measurements of electric fields of 14 V/mm were possible. We plan to continue both theoretical and experimental work in order to reduce this limit further.

ACKNOWLEDGMENTS

V.P.G. and H.J.K. were supported by the Japan Society for the Promotion of Science, and the research project was supported partially by a grant-in-aid from the Japanese Ministry of Education, Science, Culture, and Sport. The experimental work was conducted at the Institute for Ionized Gas and Laser Research at Kyushu University. The authors are grateful to T. Yamada and K. Takeda for assistance with the experiment.

[1] J. P. Booth, M. Fadlallah, J. Derouard, and N. Sadeghi, Appl. Phys. Lett. **65**, 819 (1994).

[2] U. Czarnetzki, D. Luggenhölscher, and H. F. Döbele, Plasma Sources Sci. Technol. **8**, 230 (1999).

[3] D. K. Doughty and J. E. Lawler, Appl. Phys. Lett. **45**, 611 (1984).

[4] J. R. Shoemaker, B. N. Ganguly, and A. Garscadden, Appl. Phys. Lett. **52**, 2019 (1988).

[5] B. L. Preppernau and B. N. Ganguly, Rev. Sci. Instrum. **64**, 1414 (1993).

[6] K. E. Greenberg and G. A. Hebner, Appl. Phys. Lett. **63**, 3282 (1993).

[7] M. D. Bowden, Y. W. Choi, K. Muraoka, and M. Maeda, Appl. Phys. Lett. **66**, 1059 (1995).

[8] M. M. Kuraica and N. Konjevic, Appl. Phys. Lett. **70**, 1521 (1997).

[9] K. Takiyama, T. Katsuta, M. Watanabe, S. Li, T. Oda, T. Ogawa, and K. Mizuno, Rev. Sci. Instrum. **68**, 1028 (1997).
[10] J. B. Kim, K. Kawamura, Y. W. Choi, M. D. Bowden, and K. Muraoka, IEEE Trans. Plasma Sci. **27**, 1510 (1999).
[11] C. A. Moore, G. P. Davis, and R. A. Gottscho, Phys. Rev. Lett. **52**, 538 (1984).
[12] R. A. Gottscho, Phys. Rev. A **36**, 2233 (1987).
[13] M. D. Bowden, T. Nakamura, K. Muraoka, Y. Yamagata, B. W. James, and M. Maeda, J. Appl. Phys. **73**, 3664 (1993).
[14] H. Debontride, J. Derouard, P. Edel, R. Romestain, N. Sadeghi, and J. P. Boeuf, Phys. Rev. A **40**, 5208 (1989).
[15] M. P. Alberta, H. Debontride, J. Derouard, and N. Sadeghi, J. Phys. III **3**, 105 (1993).
[16] S. Maurmann, V. P. Gavrilenko, H.-J. Kunze, and E. Oks, J. Phys. D **29**, 1525 (1996).
[17] Y. W. Choi, M. D. Bowden, and K. Muraoka, Appl. Phys. Lett. **69**, 1361 (1996).
[18] J. B. Kim, K. Kawamura, Y. W. Choi, M. D. Bowden, K. Muraoka, and V. Helbig, IEEE Trans. Plasma Sci. **26**, 1556 (1998).
[19] G. Racah, Phys. Rev. **61**, 537 (1942).
[20] I. I. Sobelman, *Atomic Spectra and Radiative Transitions* (Springer-Verlag, Heidelberg, 1979).
[21] A. R. Edmonds, J. Picart, N. Tran Minh, and R. Pullen, J. Phys. B **12**, 2781 (1979).
[22] H. A. Bethe, and E. E. Salpeter, *Quantum Mechanics of One- and Two-Electron Atoms* (Academic, New York, 1957).
[23] P. F. Brevet, M. Pellarin, and J. L. Vialle, Phys. Rev. A **42**, 1460 (1990).